

Effects of monolayer-substrate dynamical coupling. Argon on graphite

A. D. Novaco

*Lafayette College, Easton, Pennsylvania 18042
and Brookhaven National Laboratory, Upton, New York 11973*

J. P. McTague

*University of California, Los Angeles, California 90024
and Brookhaven National Laboratory, Upton, New York 11973*

(Received 3 January 1979)

The dynamical coupling between a solid monolayer film of argon and a substrate of graphite is examined for its effect upon the inelastic neutron scattering from the combined system. A simple model is used to describe the coupled system and the problem is reduced to a calculation of the vibrational modes of a slab of finite thickness. The results show that there is a significant amount of coupling between the film and the substrate, but that the usual geometry of the neutron scattering experiments for these systems is such that this coupling does not affect the scattering intensity significantly. The result of this calculation is used to justify the background subtraction procedure which is used to determine the dynamical response of the adsorbed film. The importance of the dynamical coupling of the film and the substrate to other aspects of monolayer physics is discussed briefly.

I. INTRODUCTION

The only monolayer system whose phonon spectrum has been determined in detail is argon on the (001) surface of graphite. Neutron scattering has shown that the essential characteristics of the inelastic scattering can be understood using a model in which the graphite and the film modes are dynamically decoupled.¹ Within this approximation, the monolayer moves in the static (time averaged) field of the substrate. Because the graphite basal plane surface and the argon monolayer are incommensurate and weakly coupled, the periodic structure of the graphite has only a small effect upon the motion of the argon and the lattice dynamics of the argon can then be approximated by replacing the graphite basal planes with smooth ones. In such an approximation, the argon has three modes for every (two-dimensional) wave vector, two acoustic ones (polarized in the surface plane) and one opticlike mode (polarized in the surface-normal direction). However, a simple one-dimensional (1-D) analysis¹ showed that the substrate-monolayer dynamical coupling has some important consequences, producing a mixed (resonant) argon-graphite band since the "natural" argon surface-normal frequency lies within the graphite bulk phonon band.

A first-principles calculation of the argon-graphite system is complicated by the complex crystal structure of the graphite. However, it is quite possible to simplify the problem so that the important characteristics of this dynamical coupling are retained, while those complexities which have little bearing upon the

physics of the coupling are eliminated. These simplifications reduce the actual problem to that of surface modes in finite slabs.²⁻⁴ The normal modes and inelastic neutron scattering intensity can then be calculated in a straightforward fashion. It is found that the major effect of the dynamical coupling is to shift the opticlike shear-vertical mode downward from its rigid substrate value by 5 to 10% for those geometries usually used in neutron scattering experiments. However, this mode always appears as a well-defined peak. It is also concluded that in the limit $q \rightarrow 0$ all modes become essentially bulk ones, so the very long-wavelength motion of the monolayer atom is strongly influenced by the dynamics of the bulk material. Thus the degree to which an adsorbed monolayer can be considered to be a two-dimensional system will depend on which dynamical modes are probed by the phenomena being observed.

II. MODEL OF THE MONOLAYER-SUBSTRATE SYSTEM

The principal motive in constructing the model system is to simplify the dynamics of the graphite lattice yet retain the essential physics of the monolayer-graphite coupling. The modes in graphite which couple effectively to the argon are those whose frequencies nearly match those of the argon shear-vertical mode on a rigid substrate. Both the in-plane and the shear-vertical modes of argon have frequencies which are quite low compared to typical graphite vibrational frequencies.^{1,5} The in-plane argon modes are acoust-

ical with a maximum frequency such that $\hbar\omega \approx 6$ meV, and the shear-vertical mode spectrum for argon on a fixed substrate is essentially flat with $\hbar\omega \sim 5-6$ meV. In bulk graphite the vast majority of modes having frequencies in the 0-6 meV range are those where the carbon atoms move mainly perpendicular to the basal plane.⁵ The few low-frequency modes which involve the relative motion of the basal planes in the direction parallel to these planes occupy a very small portion of phase space. This structure is a consequence of the extremely anisotropic nature of graphite, with relatively stiff basal planes loosely coupled to each other. Since the intraplane coupling constants are much larger than the interplane coupling constants, most eigenvectors in the Brillouin zone will be essentially polarized either in the direction parallel to the plane or that normal to it. Furthermore, the softer modes are almost all associated with the surface normal motion implying that oscillations in this direction will have the larger amplitudes. With all this in mind, we will simplify the dynamics of the graphite lattice by decoupling the in-plane and surface-normal motion and focus our attention on the latter.

The argon layer is known to be incommensurate with the graphite lattice. Therefore it is reasonable to assume that the exact crystal structure of the graphite will not have an important role to play in the dynamical coupling of monolayer and substrate modes. The obvious simplification is to choose the crystal structure of the model substrate to be the same as that of the monolayer. Such an approach is justified if the monolayer-substrate two-body potential is relatively smooth, and the important coupling is near the zone center. Both conditions appear to hold in the argon-graphite case. The mass of the model substrate atom is fixed to give the same mass per unit area as the graphite basal planes. The substrate coupling constants are then chosen to produce the same dispersion curves as the graphite lattice for frequencies near those of the monolayer. The spacing between all substrate planes and between the monolayer and substrate is chosen to be equal to the distance between the graphite basal planes. (This is in agreement with calculations based upon model potentials.)

The scattering length for the model substrate atom was chosen to reproduce the $q \rightarrow 0$ scattering intensity of graphite.⁶ The model for the argon-graphite system then consists of a finite set of parallel planes, the atoms in each plane constrained to move in the surface-normal direction only. The first plane ($\nu=0$) represents the argon monolayer and consists of atoms with mass $\mu_0=36$ u and scattering length $b_0=23.4$ fm. These atoms are arranged in a simple hexagonal array with lattice constant $a=0.386$ nm. The other planes ($\nu=1, \dots, N$) consist of atoms with mass $\mu_1=60$ u and scattering length $b_1=40.0$ fm. The atoms in the planes with $\nu \geq 1$ have the same

configuration as those in the $\nu=0$ plane. All planes are spaced a distance $d=0.334$ nm apart.

The dynamical matrix for the above system is an $N+1$ by $N+1$ matrix which is a function of q_{\parallel} , the wave vector in the plane. It is useful to define a set $q_{\perp} = (\pi/d)(n/N)$ (where $n=0, 1, \dots, N$ is the mode index at fixed q_{\parallel} ordered from lowest to highest frequency). In this $N+1$ layer system, q_{\perp} plays a role similar to that of the wave vector along the C axis in bulk graphite. Bulk modes along high-symmetry directions correspond to $q_{\parallel}=0$, $q_{\perp}=0$, or $q_{\perp}=\pi/d$. The model thus includes the equivalent of bulk modes propagating in all directions but with polarization vectors now constrained to being in the direction \perp to the surface.

There are five coupling constants (ϕ_1 thru ϕ_5) used in the calculation. These are illustrated in Fig. 1. Let j be the index for the 2-D hexagonal lattice and ν be the index for the planes. The intraplane nearest-neighbor coupling constant for $\nu=0$ is denoted by ϕ_1 . The coupling between the monolayer and substrate is represented by ϕ_2 which couples the $\nu=0$ and $\nu=1$ planes at lattice sites with the same j index. There is no second-nearest-neighbor coupling between the $\nu=0$ and $\nu=1$ plane because the argon lattice is incommensurate with the graphite lattice. The existence of such an interaction would "pin" the two lattices together and be inconsistent with the invariance of the potential energy to translations of the two incommensurate lattices. The nearest-neighbor intraplane couplings in all planes with $\nu \geq 1$ are represented by ϕ_3 . The interplane coupling constant ϕ_4 represents the interactions between nearest-neighbor

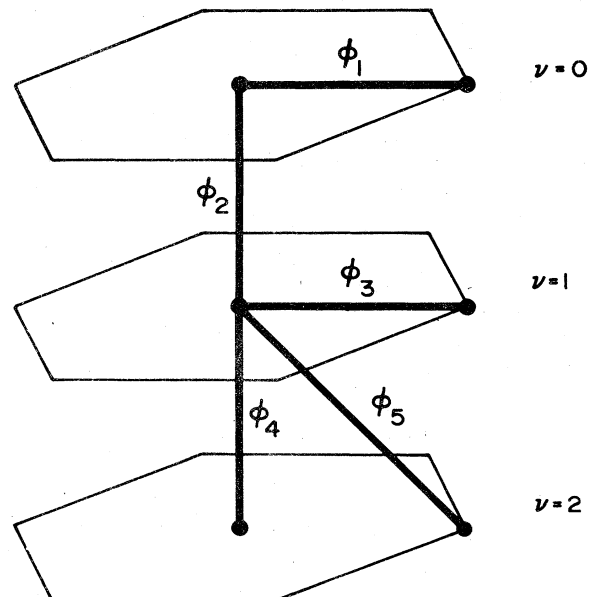


FIG. 1. Diagram for force constants of monolayer-substrate model. The $\nu=0$ plane represents the monolayer while the $\nu=1$ to N planes represent the substrate.

atoms in adjacent layers, while ϕ_5 represents the corresponding next-nearest-neighbor interactions. In Table I we list the resultant dynamical matrix $D^{\nu\nu}(q)$. Normal mode frequencies $\omega(q_{\parallel})$ and eigenvectors $\epsilon^{\nu}(q_{\parallel})$ are then given by

$$D^{\nu\nu}(\bar{q}_{\parallel}) \epsilon^{\nu}(\bar{q}_{\parallel}) = \omega^2(\bar{q}_{\parallel}) \epsilon^{\nu}(\bar{q}_{\parallel}) . \quad (1)$$

$$I(\bar{Q}, \omega) = N \left[\frac{\hbar^2}{2a^2} \right] \left[1 - \frac{\hbar\omega}{E_0} \right]^{1/2} Q_{\perp}^2 \sum_{\nu} \frac{1}{\hbar\omega_{\nu}(Q_{\parallel})} [f_{\nu}^2(\bar{Q}) + \tilde{f}_{\nu}^2(\bar{Q})] \frac{1}{\hbar\sigma(2\pi)^{1/2}} \exp \left[-\frac{1}{2} \left(\frac{\omega - \omega_{\nu}(\bar{Q}_{\parallel})}{\sigma} \right)^2 \right] , \quad (2)$$

where Q_{\perp} and Q_{\parallel} are the surface-normal and in-plane components of the scattering vector, E_0 is the energy of the incoming neutron, σ is the frequency spread of the Gaussian, and the form factors $f_{\nu}(\bar{Q})$ and $\tilde{f}_{\nu}(\bar{Q})$ are given by

$$f_{\nu}(\bar{Q}) = \sum_{\nu} \frac{b_{\nu}}{(\mu_{\nu})^{1/2}} \epsilon^{\nu}(\bar{Q}_{\parallel}) \cos(\nu d Q_{\perp}) , \quad (3a)$$

$$\tilde{f}_{\nu}(\bar{Q}) = \sum_{\nu} \frac{b_{\nu}}{(\mu_{\nu})^{1/2}} \epsilon^{\nu}(\bar{Q}_{\parallel}) \sin(\nu d Q_{\perp}) ,$$

where

$$b_{\nu} = b_0, \quad \mu_{\nu} = \mu_0, \quad \text{for } \nu = 0$$

and

$$b_{\nu} = b_1, \quad \mu_{\nu} = \mu_{\nu}, \quad \text{for } \nu \geq 1 \quad (3b)$$

TABLE I. Matrix elements of the dynamical matrix.

$$D^{00}(\bar{q}) = \frac{1}{\mu_0} [\phi_1 f_1(\bar{q}) + \phi_2]$$

$$D^{01}(\bar{q}) = \frac{-1}{(\mu_0 \mu_1)^{1/2}} \phi_2$$

$$D^{11}(\bar{q}) = \frac{1}{\mu_1} [\phi_3 f_1(\bar{q}) + \phi_4 + 6\phi_5 + \phi_2]$$

$$D^{0\nu} = 0, \quad \nu \geq 2$$

$$D^{12}(\bar{q}) = \frac{-1}{\mu_1} [\phi_4 + \phi_5 f_2(\bar{q})]$$

$$D^{22}(\bar{q}) = \frac{1}{\mu_1} [\phi_3 f_1(\bar{q}) + 2\phi_4 + 12\phi_5]$$

$$D^{\nu\nu}(\bar{q}) = D^{12}(\bar{q}) \delta_{\nu, \nu-1}, \quad \nu \geq 1$$

$$D^{\nu\nu}(\bar{q}) = D^{22}(\bar{q}), \quad \nu \geq 2$$

$$f_1(\bar{q}) = 6 - 2 \cos(q_x a) - 4 \cos\left(\frac{1}{2} q_x a\right) \cos\left(\frac{\sqrt{3}}{2} q_y a\right)$$

$$f_2(\bar{q}) = 2 \cos(q_x a) + 4 \cos\left(\frac{1}{2} q_x a\right) \cos\left(\frac{\sqrt{3}}{2} q_y a\right)$$

The scattering law (differential scattering cross section) for the system is calculated from the frequencies and polarization vectors of the normal modes, and its single-phonon contribution is folded with a Gaussian resolution function to represent the finite resolution of the experiment. $I(\bar{Q}, \omega)$ (the scattering intensity) is then given by⁷

III. RESULTS

The five coupling constants ϕ_1 through ϕ_5 are determined by the "bare" frequencies and these are known. Thus, within the framework of our model, the importance of the dynamical coupling between argon and graphite is completely determined by the frequency spectrum of bare graphite,⁵ the frequency of a single argon atom on a fixed graphite substrate,⁸ and the argon-argon Lennard-Jones interaction.⁹ The value of ϕ_1 can be estimated from the known Lennard-Jones interaction between argon atoms and the lattice constant of 0.386 nm, giving $\phi_1 \approx 100$ meV/nm². The value of ϕ_2 was chosen to be 21500 meV/nm² since this given as Einstein oscillator frequency for argon (on a rigid graphite substrate) with $\hbar\omega = 5.0$ meV. An upper limit for ϕ_2 is about 25000 meV/nm², but the results are not altered in any significant manner by 10 or 20% variations. Since $\phi_1 \ll \phi_2$ the dispersion curve for the argon mode is very flat, and we can set $\phi_1 = 0$ with no significant effect. The values of ϕ_3 , ϕ_4 , and ϕ_5 were determined by trial and error fitting of the model dispersion curves to the measured ones for graphite.⁵ A good fit was obtained with $\phi_3 = 21500$ meV/nm², $\phi_4 = 102500$ meV/m², and $\phi_5 = -2100$ meV/nm². Figure 2 shows the model spectrum versus that for graphite, plotted as a function of \bar{q}_{\parallel} . The model and experimental frequencies are in very close agreement in the physically important region ($\hbar\omega < 7$ meV). The graphite modes not represented in our model are those which exist between the LO and LA curves for $q_{\parallel} \neq 0$. These represent modes whose polarization is essentially parallel to the basal plane and whose frequencies are very high except for a very small region just around $q_{\parallel} = 0$ (as can be seen from Fig. 2.) This region makes a negligible contribution to the calculated scattering intensities since these are averaged over the whole Brillouin zone. Thus, we do not make any significant error in ignoring them.

Figure 3 shows the calculated curves for the substrate with a monolayer of argon on the surface. The only modes which are plotted are the shear-vertical

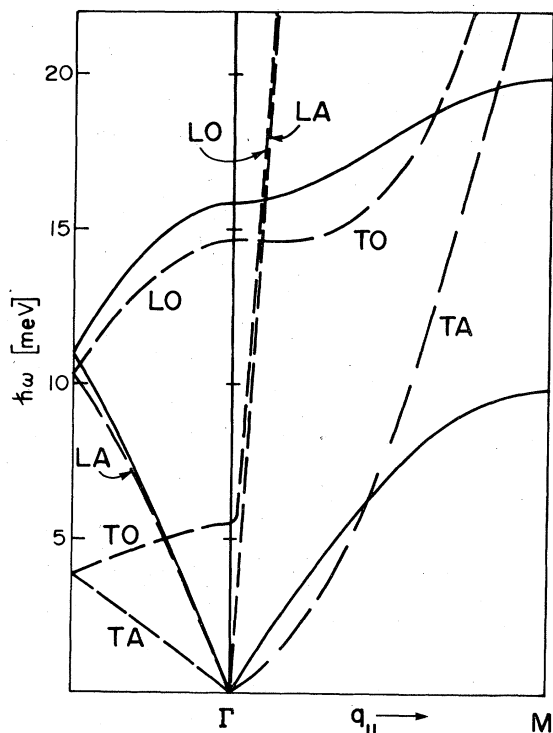


FIG. 2. Calculated mode frequencies for model without monolayer (—) vs calculated mode frequencies for bulk graphite (---) as given in Ref. 5. These modes are plotted as a function of \bar{q}_{\parallel} , the only true \bar{q} vector for the slab. Between Γ and M we show the lowest- and highest-frequency modes for both systems. To the left of Γ are shown all the modes for $\bar{q}_{\parallel}=0$. For the bulk system this axis represents q_{\perp} and the far left boundary is $q_{\perp}=\pi/2c$ where c is the length of the graphite unit cell along the c axis. For the model, this axis represents the mode index n with the lower branch representing $(0 < n \leq \frac{1}{2}N)$ plotted with n increasing to the left and with the upper branch representing $(\frac{1}{2}N \leq n < N)$ plotted with n increasing to the right.

modes which are primarily adatom ones (labeled SV), the lowest substrate mode (labeled TA) and the highest substrate one (labeled TO). Where the SV and TA modes merge in q space, several eigenvectors contribute to the motion of the argon. The modes at smaller \bar{q}_{\parallel} have strongly mixed bulk plus surface character. Figure 4 shows the contributions made to the argon's motion by modes with $\bar{q}_{\parallel}=0$, and $\bar{q}_{\parallel}=\bar{q}_1$, where \bar{q}_1 is the \bar{q} vector at which the argon mode merges with the bulk (labeled point A). The SV modes at higher \bar{q} rapidly assume pure argon character. Thus the dynamical coupling is strongest at the zone center, weak at \bar{q}_1 , and negligible at the zone boundary. Since the modes are strongly coupled only over a rather small region in the Brillouin zone (centered about the Γ point), the $I(\bar{Q}, \omega)$ func-

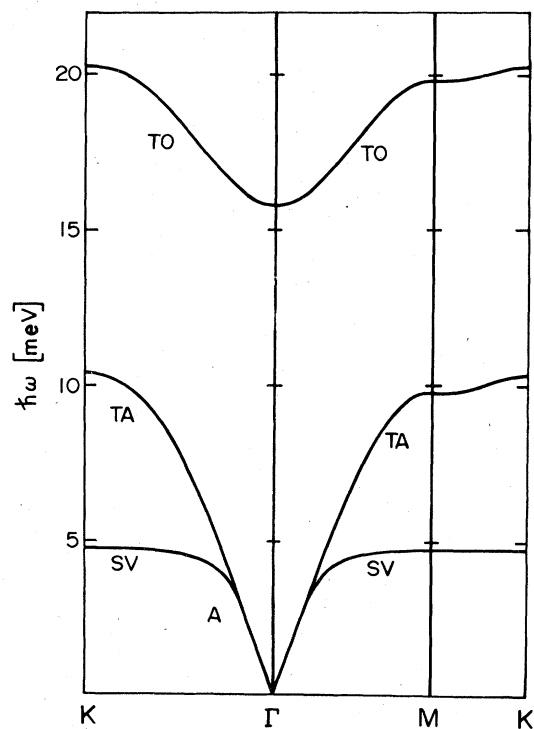


FIG. 3. Selected mode frequencies calculated for model with monolayer. Between the TA and TO branches there are $N-2$ closely spaced modes which are essentially bulk modes. A is the point where the monolayer mode merged with the bulk modes.

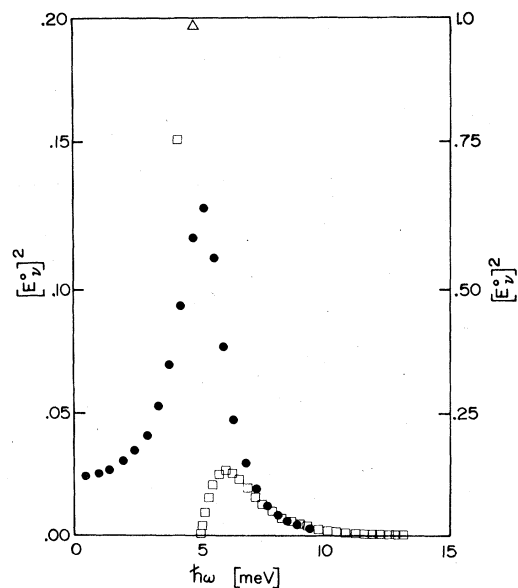


FIG. 4. Weighting factor for monolayer motion for three sets of modes. Each set consists of all the modes at some fixed \bar{q}_{\parallel} with (\bullet) being at $\bar{q}_{\parallel}=0$, (\square) at point A on Fig. 3, and (Δ) at the zone boundary. The right-hand scale is for the top two points (Δ and \square), while all other points should be read from the left.

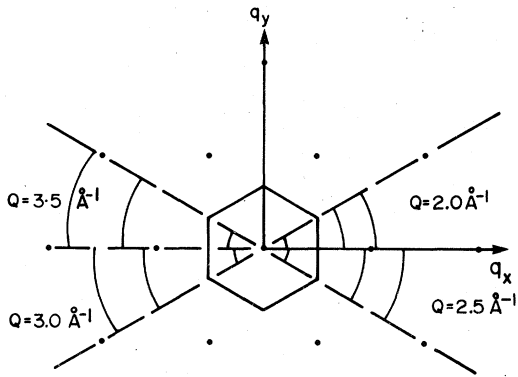


FIG. 5. Selected paths in $\bar{q}_{||}$ space used in the calculation at $I(\bar{Q}, \omega)$. Each filled circle represents a reciprocal lattice point and the average over ϕ (the azimuthal angle) for fixed θ (the polar angle) is calculated over a given arc. The innermost arc is for $\theta = 10^\circ$, the middle arc is for $\theta = 45^\circ$ and the outermost arc is for $\theta = 80^\circ$.

tion when averaged over a typical experimental orientational distribution does not directly reveal this coupling, but rather shows a distinct Einstein oscillator signal having a peak with energy 10 to 20% below the Einstein value $(\hbar^2 \phi_3 / \mu_0)^{1/2}$. Thus the dynamical interaction with the substrate renormalizes the argon Einstein oscillator frequency.

$I(\bar{Q}, \omega)$ was calculated for four values of \bar{Q} (2.0, 2.5, 3.0, and 3.5 \AA^{-1}) chosen for comparison with published experiments.¹ In all cases this function was averaged over ϕ , the orientation angle of \bar{Q} about the C axis. Calculations were done for both

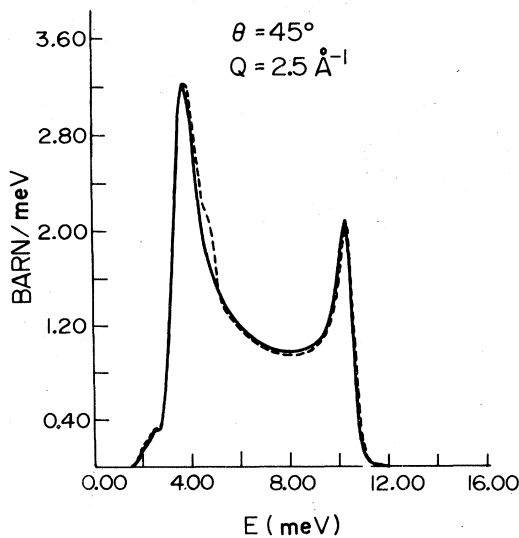


FIG. 6. Scattering cross section $I(\bar{Q}, \omega)$ for $Q = 2.5 \text{ \AA}^{-1}$ and $\theta = 45^\circ$, averaged over ϕ , for the pure substrate (—) and for the monolayer-substrate combination (----).

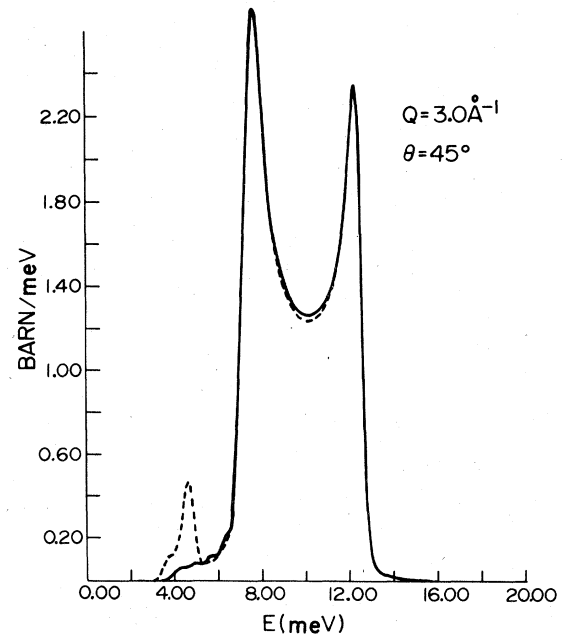


FIG. 7. Scattering cross section $I(\bar{Q}, \omega)$ for $Q = 3 \text{ \AA}^{-1}$ and $\theta = 45^\circ$, averaged over ϕ , for the pure substrate (—) and for the monolayer substrate combination (----).

fixed θ (where θ is the angle of \bar{Q} relative to the C axis) and for $I(\bar{Q}, \omega)$ averaged over values of θ . Fixed θ calculations were done at $\theta = 10, 45$, and 80° . Figure 5 shows the path of the $\bar{q}_{||}$ vector in reciprocal space for fixed θ . Note that the large \bar{Q} values used result in little weight being given to those points in q space where dynamical coupling is impor-

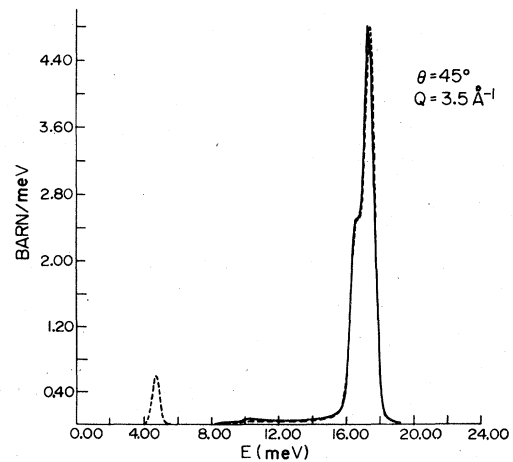


FIG. 8. Scattering cross section $I(\bar{Q}, \omega)$ for $Q = 3.5 \text{ \AA}^{-1}$ and $\theta = 45^\circ$, averaged over ϕ , for the pure substrate (—) and for the monolayer-substrate combination (----).

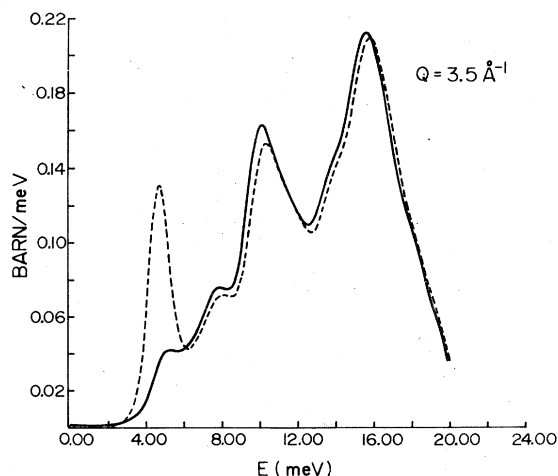


FIG. 9. Scattering cross section $I(\bar{Q}, \omega)$ for $Q = 3.5 \text{ \AA}^{-1}$, averaged over ϕ and partially over θ . This powder average simulates Ar on the partially oriented substrate Grafoil. (---) Ar + graphite; (—) graphite alone.

tant. Typical scans are shown in Figs. 6 – 9, demonstrating how the Einstein oscillator response always appears in the difference spectrum. In fact, Fig. 6 was chosen because it was a "worst case", yet the difference signal still shows the Einstein oscillator peak. While there are interference and dynamical coupling effects these are very difficult to discern, and under typical experimental conditions only the single peak would be seen. The major consequence of dynamical coupling is the 10 to 20% shift to lower frequency, indicating that the experimental data should be shifted up by a similar factor if the cou-

pling constant is to be determined by the inelastic scattering intensity.

In the final analysis, this calculation demonstrates the validity of the background subtraction used in the experiments to determine the rare-gas "monolayer" signal when the substrate is graphite. Obviously, very careful experiments combined with model calculations could result in information being obtained concerning these interference and coupling effects, but it will be very difficult to do so with any reasonable degree of accuracy. Finally, it should be noted that the one group of modes which couple to the bulk ones is just that which tends to make two-dimensional systems special, namely, the group of very long-wavelength phonons. Even though we have not carried out calculations for the in-plane modes, their physics will be much the same as the shear-vertical mode we have investigated. That is, at very long wavelengths they will nearly match the bulk modes in frequency and will couple to them. Thus, it can be said that there are no truly 2-D long-wavelength phonons in these monolayer systems, but only some approximation to them with the 2-D approximation eventually becoming invalid for very long wavelengths. What consequences this might have on phase transitions in monolayer systems is a provocative question which we leave unanswered.

ACKNOWLEDGMENTS

This research was supported in part by NSF under Grants No. DMR75-15630 (A.D.N.) and No. CHE76-21293 (J.P.M.). Research at Brookhaven supported in part by the Division of Basic Energy Sciences, DOE, under Contract No. ET-76-C-02-0016.

¹H. Taub, K. Carneiro, J. K. Kjems, L. Passell, and J. P. McTague, *Phys. Rev. B* **16**, 4551 (1977).

²R. E. Allen, G. P. Alldredge, and F. W. deWette, *Phys. Rev. B* **4**, 1648 (1971); **4**, 1661 (1971); **4**, 1682 (1971).

³W. R. Lawrence and R. E. Allen, *Phys. Rev. B* **14**, 2910 (1976); and R. E. Allen and W. R. Lawrence, *Phys. Rev. B* **15**, 5081 (1977).

⁴B. Djafari-Rovhani and L. Dobrzynski, *J. Phys. (Paris)* **38**, C4-126 (1977).

⁵R. Nicklow, N. Wakabayashi, and H. G. Smith, *Phys. Rev. B* **5**, 4951 (1972).

⁶G. E. Bacon, *Neutron Diffraction* (Clarendon, Oxford, 1975).

⁷W. M. Lomer and G. C. Low, in *Thermal Neutron Scattering*, edited by P. A. Egelsteff (Academic, London, 1965).

⁸W. A. Steele, *Surf. Sci.* **36**, 317 (1973).

⁹G. K. Horton, in *Rare Gas Solids*, edited by M. L. Klein and J. A. Venables (Academic, New York, 1976), Vol. 1, p. 88.